

Turbulent transport in tokamak plasmas with rotational shear

M. Barnes,^{1,2,*} F. I. Parra,¹ E. G. Highcock,^{1,2} A. A. Schekochihin,¹ S. C. Cowley,² and C. M. Roach²

¹*Rudolf Peierls Centre for Theoretical Physics, University of Oxford, 1 Keble Road, Oxford OX1 3NP, UK*

²*Euratom/CCFE Fusion Association, Culham Science Centre, Abingdon OX14 3DB, UK*

Nonlinear gyrokinetic simulations have been conducted to investigate turbulent transport in tokamak plasmas with rotational shear. At sufficiently large flow shears, linear instabilities are suppressed, but transiently growing modes drive subcritical turbulence whose amplitude increases with flow shear. This leads to a local minimum in the heat flux, indicating an optimal $\mathbf{E} \times \mathbf{B}$ shear value for plasma confinement. Local maxima in the momentum fluxes are also observed, allowing for the possibility of bifurcations in the $\mathbf{E} \times \mathbf{B}$ shear. The sensitive dependence of heat flux on temperature gradient is relaxed for large flow shear values, with the critical temperature gradient increasing at lower flow shear values. The turbulent Prandtl number is found to be largely independent of temperature and flow gradients, with a value close to unity.

Introduction. Experimental measurements in magnetic confinement fusion devices indicate that sheared mean $\mathbf{E} \times \mathbf{B}$ flows can significantly reduce and sometimes fully suppress turbulent particle, momentum, and heat fluxes [1, 2]. Since these turbulent fluxes determine mean plasma density and temperature profiles, their reduction leads to a local increase in the profile gradients. This increase can be dramatic: transport barriers in both the plasma core and edge have been measured with radial extents on the order of only tens of ion Larmor radii [3]. The associated increase in core density and temperature results in increased fusion power. Thus, understanding how shear flow layers develop and what effect they have on turbulent fluxes is both physically interesting and practically useful.

This Letter reports a numerical study of the influence of sheared toroidal rotation on turbulent heat and momentum transport in tokamak plasmas. Two main effects of sheared toroidal rotation were identified in previous numerical work [4–8]: suppression of turbulent transport by shear in the perpendicular (to the mean magnetic field) velocity and linear destabilization due to the parallel velocity gradient (PVG). While the former observation indicates that a finite flow shear improves plasma confinement, the latter raises the question of whether more shear is always beneficial. Below we report that the PVG-driven linear instability [9] is stabilized at sufficiently large flow shear values, consistent with fluid theory in slab geometry [10]. Correspondingly, fluxes decrease with increasing flow shear as the linear stabilization point is approached. However, beyond this point, transiently growing modes driven by the PVG give rise to subcritical turbulence. The fluxes associated with this turbulence increase with flow shear. This implies an optimal flow shear for each temperature gradient; the fact that the minimum heat flux value is finite indicates that there is a maximum attainable temperature gradient that can be maintained for a given heat flux. Additionally, the observed presence of maxima in the momentum fluxes admits the possibility of bifurcations in the flow shear (and thus the temperature gradient).

In the absence of flow shear, a small increase in temperature gradient leads to a large increase in heat flux (“stiff transport”). Recent experimental evidence [11] suggests that flow shear may reduce this sensitivity in configurations with low magnetic shear. Our results indicate that at low flow shear values, both the critical temperature gradient for the onset of turbulence and the stiffness increase. At high flow shear values, the opposite behavior is observed (the stiffness and critical temperature gradient both decrease).

Model. A closed set of evolution equations [12, 13] for mean plasma density, pressure, and toroidal angular momentum is obtained by taking moments of the kinetic equation and applying the δf gyrokinetic ordering [14, 15]. These moment equations relate the evolution of the mean quantities to particle, momentum, and heat fluxes, which are typically dominated by turbulent contributions. We restrict our attention to electrostatic fluctuations and assume a modified Boltzmann response [16] for the electron distribution. The resultant particle flux is identically zero, and the radial components of the turbulent heat flux of species s , Q_s , and toroidal angular momentum flux, Π , are given by

$$Q_s = \overline{\int d^3\mathbf{v} \left(\frac{m_s v^2}{2} \right) \left(\mathbf{v}_E \cdot \frac{\nabla\psi}{|\nabla\psi|} \right) \delta f_s} \quad (1)$$

$$\Pi = \sum_s m_s R^2 \overline{\int d^3\mathbf{v} (\mathbf{v} \cdot \nabla\phi) \left(\mathbf{v}_E \cdot \frac{\nabla\psi}{|\nabla\psi|} \right) \delta f_s}, \quad (2)$$

where ψ is a flux-surface label, ϕ the toroidal angle, m_s the particle mass, \mathbf{v} its velocity in the frame of mean flow, R its major radius, \mathbf{v}_E the fluctuating $\mathbf{E} \times \mathbf{B}$ drift velocity, δf_s the deviation of the distribution function from a local Maxwellian, and the overline denotes a spatial average over a thin annular region encompassing a given flux surface.

The distribution function δf_s appearing in Eqs. (1) and (2) is calculated by solving the standard δf gyrokinetic equation in the limit where the plasma flow speed, u , is ordered comparable to the ion thermal speed,

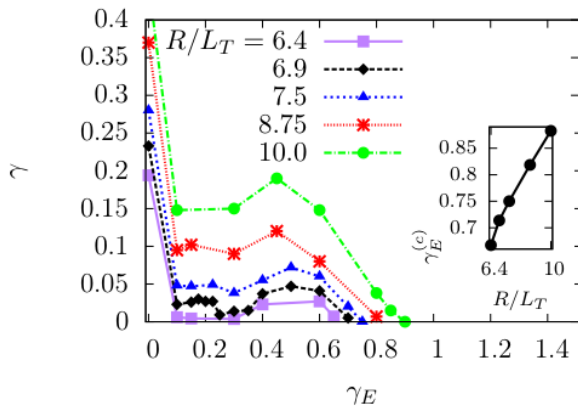


FIG. 1: Average linear growth rates vs. flow shear for different values of R_0/L_T . Inset: critical flow shear vs. R_0/L_T .

v_{th} [13, 17]. In this “high-flow” regime, the flow velocity is constrained to be $\mathbf{u} = R^2\omega(\psi)\nabla\phi$, where R is the major radius and ω is the rotational frequency [18]. We consider a subsidiary expansion in low Mach number M ($\rho_i/L \ll M \ll 1$), where L is a typical macroscopic length scale (e.g., the minor radius of the torus) and ρ_i is the ion Larmor radius. However, we allow for flow gradients of order $1/ML$, and so neglect terms proportional to ω (such as Coriolis and centrifugal drifts) but retain those proportional to $d\omega/d\psi$ (flow shear). The resulting equation is

$$\begin{aligned} \frac{dh}{dt} + \left(v_{\parallel}\hat{\mathbf{b}} + \mathbf{v}_B + \langle \mathbf{v}_E \rangle_{\mathbf{R}} \right) \cdot \nabla h - \langle C[h] \rangle_{\mathbf{R}} = \\ - \langle \mathbf{v}_E \rangle_{\mathbf{R}} \cdot \nabla \psi \left(\frac{dF_0}{d\psi} + \frac{mv_{\parallel}}{T} \frac{RB_{\phi}}{B} \frac{d\omega}{d\psi} F_0 \right) + \frac{eF_0}{T} \frac{d\langle \varphi \rangle_{\mathbf{R}}}{dt}, \end{aligned} \quad (3)$$

where $d/dt = \partial/\partial t + \mathbf{u} \cdot \nabla$, $h = \delta f + (e\varphi/T)F_0$ is the deviation of δf from a Boltzmann response, e is particle charge, φ is the electrostatic potential, $\mathbf{v}_E = (c/B^2)\mathbf{B} \times \nabla\varphi$, T is temperature, F_0 is a Maxwellian distribution of peculiar velocities, C is the collision operator, B is the magnetic field strength (with B_{ϕ} the toroidal component), $\mathbf{v}_B = \hat{\mathbf{b}}/\Omega \times \left(v_{\parallel}^2\hat{\mathbf{b}} \cdot \nabla\hat{\mathbf{b}} + v_{\perp}^2\nabla B/2B \right)$ contains magnetic drifts, Ω is the Larmor frequency, $\hat{\mathbf{b}} = \mathbf{B}/B$, and $\langle \cdot \rangle_{\mathbf{R}}$ denotes the average over gyro-angle at fixed guiding center position \mathbf{R} .

Eq. (3) is solved in the rotating reference frame using the local, nonlinear gyrokinetic code **GS2** [8, 19]. The toroidal velocity is expanded in ψ about its value at the center of the simulation domain, ψ_0 , giving $\mathbf{u} \approx R^2(\psi - \psi_0)(d\omega/d\psi)\nabla\phi$. The local approximation assumes that $d\omega/d\psi$ is constant across the simulation domain. Consequently, the effect of sheared flow is accounted for by a single parameter, $\gamma_E = (\psi/q)(d\omega/d\psi)R_0/v_{\text{th}} = (M/q)(d\ln\omega/d\ln r)$, where q is the safety factor, R_0 is the major radius at the center of the flux surface, and r

is the half-diameter of the flux surface (both measured at the height of the magnetic axis).

We study a system whose magnetic geometry corresponds to the widely-used Cyclone base case [20] (unshifted, circular flux surface with $q = 1.4$, magnetic shear $\hat{s} = d\ln q/d\ln r = 0.8$, $r/R_0 = 0.18$, and $R_0/L_n = 2.2$, with $L_n^{-1} = -d\ln n/dr$). The $\mathbf{E} \times \mathbf{B}$ shearing rate, γ_E , and the normalized inverse temperature gradient scale length, $\kappa \equiv R_0/L_T$, were varied over a wide range of values in a series of linear and nonlinear simulations.

Linear stability. The average linear growth rates, γ , obtained from these simulations are given in Fig. 1. We see that γ decreases rapidly with γ_E for small values of γ_E before increasing to a local maximum and subsequently decreasing to zero. For $\gamma_E \gtrsim 0.25$, the system is linearly unstable only in the presence of both temperature and parallel flow gradients (cf. [5–8]). The system becomes linearly stable for large values of γ_E , with the critical γ_E for stability, $\gamma_E^{(c)}$, increasing approximately linearly with κ . Beyond $\gamma_E^{(c)}$, there are no linearly unstable modes. This result is qualitatively similar to the prediction from fluid theory in a slab [10], where no linear instability is possible when γ_E/\hat{s} exceeds a certain critical value.

Heat flux. The turbulent heat flux calculated from nonlinear simulations is given in Fig. 2. For all κ values, the heat flux qualitatively follows the same trend as growth rates when $\gamma_E < \gamma_E^{(c)}$. For $\gamma_E > \gamma_E^{(c)}$, nonlinear simulations initialized with low-amplitude noise develop no turbulent transport. However, for finite initial fluctuation amplitudes, one finds that the turbulence does not necessarily decay away: for sufficiently large values of κ and initial amplitude, the flux reaches steady state values in excess of those found for γ_E just below $\gamma_E^{(c)}$ [21]. The flux then increases monotonically with γ_E . For the range of γ_E considered here, the heat flux associated with a given temperature gradient is thus minimized at a finite shearing rate.

Subcritical turbulence. Because the turbulence is present in the absence of linear instability, we refer to it as subcritical. When $\gamma_E > \gamma_E^{(c)}$, linear simulations exhibit transient growth, with order unity increases in the initial fluctuation amplitudes over times of several R_0/v_{th} before subsequent decay (Fig. 3). The duration of growth decreases with increasing flow shear, but the transient growth rate increases so that the amplification factor of the initial perturbation amplitude grows with flow shear (cf. [10]). This transient amplification provides an energy source for the turbulence, which can be maintained by the nonlinearity through redistribution of energy amongst other modes. We have identified the PVG term in Eq. 3 (the $d\omega/d\psi$ term on the RHS) as the driver of the subcritical turbulence, as the latter is no longer present when the PVG is artificially set to zero.

Momentum flux. The toroidal angular momentum flux also mimics the linear growth rate, except near $\gamma_E =$

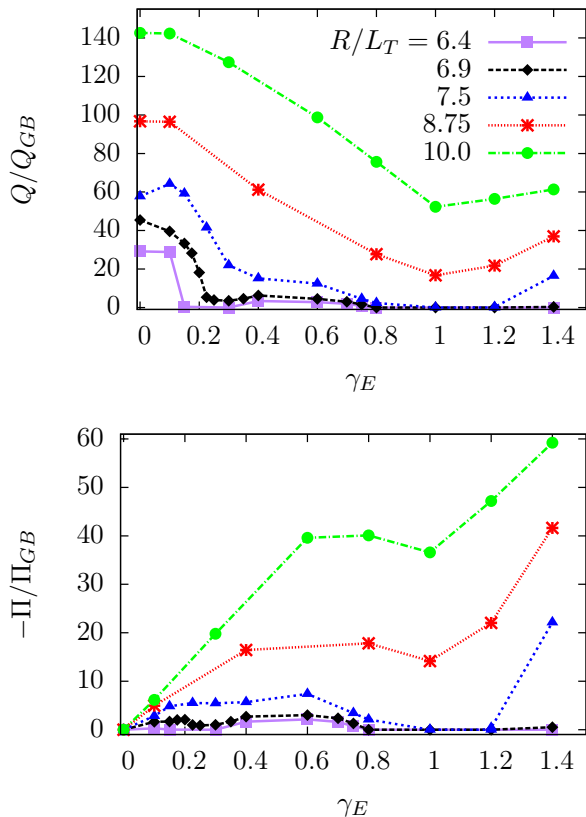


FIG. 2: Turbulent heat (top) and toroidal angular momentum (bottom) fluxes vs. flow shear for various values of R_0/L_T . For $\gamma_E \lesssim 0.25$, the heat flux is reduced by $E \times B$ shear. Beyond this value, the PVG drives instability and both heat and momentum fluxes increase. For $\gamma_E > \gamma_E^{(c)}$, the turbulence is subcritical, sustained by transiently growing modes.

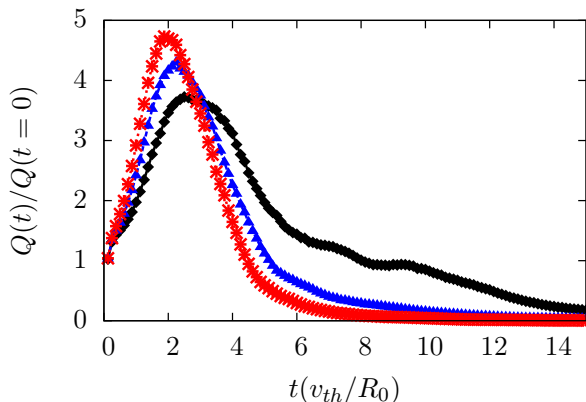


FIG. 3: Heat flux versus time obtained from linear simulations for $R_0/L_T = 8.75$ and three γ_E values at which subcritical turbulence is observed.

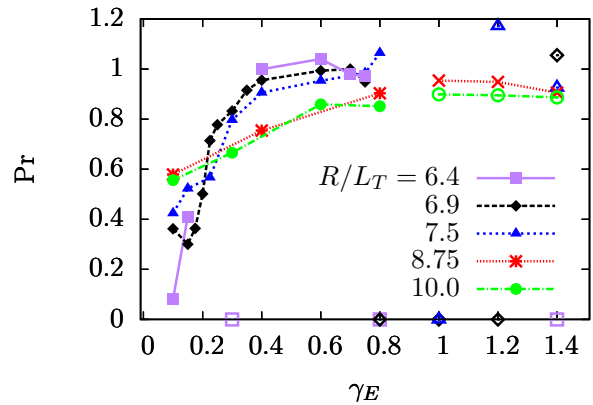


FIG. 4: Turbulent Prandtl number as a function of flow shear for various values of R_0/L_T . Unfilled points correspond to linearly stable flow shear values. Zero Pr points represent fully suppressed turbulence.

0 [22]. This is understood by expressing the momentum flux in diffusive form: $\Pi = -m_i v_{th}(qR_0/r)\nu_i(\kappa, \gamma_E)\gamma_E$, where ν_i is the turbulent viscosity. For γ_E small, the fluctuation amplitudes vary little, so ν_i is approximately constant and $\Pi \propto \gamma_E$. For larger γ_E , turbulent amplitudes drop rapidly so that Π decreases, resulting in the local maxima seen in Fig. 2. This suppression of Π is due to linear stabilization as γ_E approaches $\gamma_E^{(c)}$ from below. The momentum flux then increases monotonically when $\gamma_E > \gamma_E^{(c)}$ due to subcritical turbulence. The maxima in Π may lead to a bifurcation in flow shear, discussed in the Conclusions.

Prandtl number. The turbulent Prandtl number can be calculated from the values of Q_i and Π . It is defined as $Pr = \nu_i/\chi_i$, where the turbulent thermal diffusivity, χ_i , is given by $Q_i = -\chi_i dT_i/dr$. Fig. 4 shows that Pr is approximately independent of κ and only has strong dependence on γ_E for small values of γ_E [23]. This is despite the fact that both ν_i and χ_i individually have strong dependencies on κ and γ_E . For $\gamma_E \gtrsim 0.4$ the Prandtl number is close to unity, in good agreement with experimental measurements at low Mach numbers [24].

Stiff transport. A serious impediment to confinement is the sensitive dependence of the heat flux on small changes in κ . This stiffness of the transport makes it difficult to increase κ , and therefore the core temperature, beyond the critical value, κ_c , at which turbulence is excited. Recent experimental results indicate that stiffness, $dQ_i/d\kappa$, may be reduced at low magnetic shear, \hat{s} , and large values of γ_E [11]. For the Cyclone base case considered here ($\hat{s} = 0.8$), we find a complicated dependence of stiffness on flow shear, as illustrated in Fig. 5. At low values of γ_E ($\lesssim 0.3$), the critical κ shifts to higher values, but the stiffness increases. This makes sense intuitively: one expects that for $\kappa/\gamma_E \rightarrow \infty$, the heat flux will tend to the curve corresponding to $\gamma_E = 0$. For this

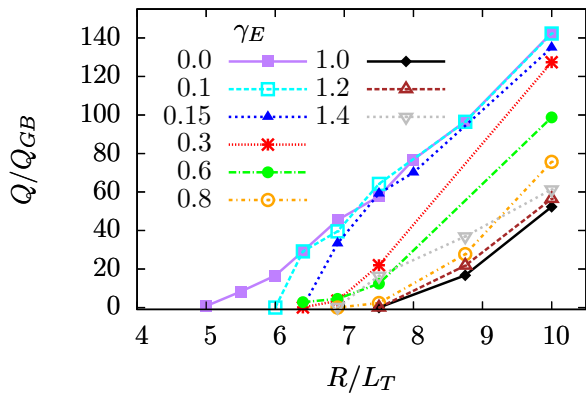


FIG. 5: Turbulent heat flux vs R_0/L_T for various values of the flow shear. Though there is some minimal relaxation of the profile stiffness for $0.3 \lesssim \gamma_E \lesssim 0.8$, the predominant effect of the shear is to shift the critical temperature gradient.

to happen, the value of $dQ_i/d\kappa$ at $Q_i = 0$ must increase to compensate for the increase in κ_c .

For $0.3 \lesssim \gamma_E < \gamma_E^{(c)}$, both κ_c and the profile stiffness decrease. This is a result of a change in the nature of the linear instability, which is now driven by the PVG. The relaxation of stiffness is modest, and it only occurs for κ near κ_c . When $\gamma_E > \gamma_E^{(c)}$, κ_c initially shifts upwards with increasing γ_E , and stiffness increases for κ near κ_c . However, for even larger γ_E , both the stiffness and κ_c decrease. This is to be expected, as the subcritical turbulence is driven by the velocity, not temperature, gradient and thus has a weaker dependence on κ .

Conclusions. We have shown that PVG-driven turbulence exists at large flow shears, but only if the initial fluctuation amplitudes are sufficiently large. This has a number of potentially important implications. First, it indicates that linear stability analysis is insufficient to determine critical gradients in rotating plasmas. Furthermore, it shows that the system can undergo hysteresis: The fluxes associated with a given flow shear and temperature gradient pair depend on the path taken to obtain that pair. As an example, consider the pair $\gamma_E = 1$, $R_0/L_T = 10$. From Fig. 2, we see that if $R_0/L_T = 10$ is obtained at $\gamma_E < \gamma_E^{(c)}$ before increasing γ_E to unity, there will be large heat and momentum fluxes. In this case, there is an optimal flow shear for confinement ($\gamma_E \approx 1$) and a maximum attainable temperature gradient for a given power input. However, if $\gamma_E = 1$ is obtained at $R_0/L_T \lesssim 7.5$ before increasing R_0/L_T to ten, then the fluxes will be zero because the initial amplitude is not large enough to excite the subcritical turbulence. Thus it may be beneficial to increase flow shear on a time scale short compared to the energy confinement time.

The existence of local maxima of the toroidal angular momentum flux provides the potential for bifurcations in γ_E and corresponding bifurcations in temperature gradi-

ent. However, a detailed transport analysis is necessary to definitively observe such a bifurcation for experimentally relevant conditions. Finally, we note that the $\mathbf{E} \times \mathbf{B}$ suppression and PVG drive terms differ by a factor proportional to $(qR_0/r)(B_\phi/B)$ [8]. Thus our results, which should be qualitatively robust, may undergo considerable quantitative variation with changes in magnetic configuration.

The authors are grateful to I. G. Abel, F. J. Casson, W. Dorland, G. W. Hammett, and A. Zocco for useful discussions. M.B. was supported by the Oxford-Culham Fusion Research Fellowship. The authors also thank the Leverhulme Trust (UK) International Network for Magnetized Plasma Turbulence for travel support. Computing time for this research was provided by EPSRC grant EP/H002081/1.

* Electronic address: michael.barnes@physics.ox.ac.uk

- [1] K. H. Burrell, Phys. Plasmas **4**, 1499 (1997).
- [2] G. D. Conway et al., Phys. Rev. Lett. **84**, 1463 (2000).
- [3] G. Tresset et al., Nucl. Fusion **42**, 520 (2002).
- [4] R. E. Waltz, R. L. Dewar, and X. Garbet, Phys. Plasmas **5**, 1784 (1998).
- [5] J. E. Kinsey, R. E. Waltz, and J. Candy, Phys. Plasmas **12**, 062302 (2005).
- [6] A. G. Peeters and C. Angioni, Phys. Plasmas **12**, 072515 (2005).
- [7] F. J. Casson et al., Phys. Plasmas **16**, 092303 (2009).
- [8] C. M. Roach et al., Plasma Phys. Control. Fusion **51**, 124020 (2009).
- [9] P. J. Catto, M. N. Rosenbluth, and C. S. Liu, Phys. Fluids **16**, 1719 (1973).
- [10] S. L. Newton, S. C. Cowley, and N. F. Loureiro, Plasma Phys. Control. Fusion (2010), submitted.
- [11] P. Mantica et al., Phys. Rev. Lett. **102**, 175002 (2009).
- [12] H. Sugama and W. Horton, Phys. Plasmas **4**, 405 (1997).
- [13] I. G. Abel et al., Plasma Phys. Control. Fusion, submitted (2010).
- [14] T. M. Antonsen and B. Lane, Phys. Fluids **23**, 1205 (1980).
- [15] E. A. Frieman and L. Chen, Phys. Fluids **25**, 502 (1982).
- [16] G. W. Hammett et al., Plasma Phys. Control. Fusion **35**, 973 (1993).
- [17] M. Artun and W. M. Tang, Phys. Plasmas **1**, 2682 (1994).
- [18] F. L. Hinton and S. K. Wong, Phys. Fluids **28**, 3082 (1982).
- [19] M. Kotschenreuther, G. Rewoldt, and W. M. Tang, Comp. Phys. Comm. **88**, 128 (1995).
- [20] A. M. Dimits et al., Phys. Plasmas **7**, 969 (2000).
- [21] We have verified that this subcritical turbulence persists when kinetic electrons are included, in contrast with the qualitatively different phenomenon observed in [5].
- [22] At $\gamma_E = 0$ symmetry arguments suggest Π vanishes unless up-down asymmetry, the Coriolis drift, or other symmetry-breaking effects are included; A. G. Peeters, C. Angioni, and D. Strintzi, Phys. Rev. Lett. **98**, 265003 (2007).
- [23] In [7], which considers a different magnetic equilibrium

and flow shear values for which there is no subcritical turbulence, Pr is found to be unity and independent of γ_E for a single κ value.

[24] P. C. de Vries et al., Plasma Phys. Control. Fusion **52**, 065004 (2010).